

Numerical and Analytical Free Vibration Analysis of Composite Plate with Auxetic Core Layer and Functionally Graded Surface Layers

Kerim Gökhan AKTAŞ¹  Mehmet Ali GÜVENÇ^{2*} 

¹ Karabük Üniversitesi, Mühendislik Fakültesi, Makine Mühendisliği Bölümü, Karabük, Türkiye

² İskenderun Teknik Üniversitesi, Havacılık ve Uzay Bilimleri Fakültesi, Havacılık ve Uzay Mühendisliği Bölümü, Hatay, Türkiye

Article Info

Received: 27.11.2024

Accepted: 16.12.2024

Published: 31.12.2024

Keywords:

FG plate,
Auxetic core,
Finite element method,
Navier method,
Si₃N₄-Ni.

ABSTRACT

In this study, the free vibration behavior of a sandwich plate with a re-entrant auxetic core layer placed between two functionally graded (FG) composite surface layers are analyzed. Both analytical and numerical methods are employed under various boundary conditions to investigate the free vibration response of the three-layer sandwich structure. The FG layers are modeled using a silicon nitride (Si₃N₄)-nickel (Ni) ceramic-metal matrix, selected for its superior thermal and mechanical properties. The material properties of the re-entrant auxetic core and FG surface plates are considered temperature-dependent, allowing for a realistic representation of environmental effects. The effective material properties of the FG plates are defined using a power-law distribution, enabling a gradual variation in composition through the plate's thickness. Hamilton's principle is applied to derive the governing equations of motion for the sandwich plate, ensuring an accurate theoretical foundation. To analyze the free vibration response, the Finite Element Method (FEM) and Navier method are utilized. FEM offers flexibility for various boundary conditions (BCs), while the Navier method provides a precise analytical solution for plates with uniform conditions. Simulations explore the effects of temperature changes, the power-law index, and the auxetic core's geometric parameters on the plate's vibration behavior. The results from the analytical and numerical methods show excellent agreement, confirming the validity of the approaches used. The findings reveal that temperature variations significantly influence the natural frequencies due to changes in material stiffness. Additionally, the power-law index impacts the stiffness distribution, while the auxetic core geometry, such as cell angles and dimensions, plays a key role in modifying the plate's rigidity and free vibration response. This study concludes that by optimizing these parameters, the vibration performance of sandwich plates can be enhanced for specific operating conditions. The findings are expected to provide valuable insights for designing advanced structures in areas such as aerospace, automotive and marine industries.

Auxetik Çekirdek Katmanına ve Fonksiyonel Derecelendirilmiş Yüzey Katmanlarına Sahip Kompozit Plakanın Sayısal ve Analitik Serbest Titreşim Analizi

Makale Bilgisi

Geliş Tarihi: 27.11.2024

Kabul Tarihi: 16.12.2024

Yayın Tarihi: 31.12.2024

Anahtar Kelimeler:

FG plakası,
Auxetic çekirdek,
Sonlu elemanlar yöntemi,
Navier yöntemi,
Si₃N₄-Ni.

ÖZET

Bu çalışmada, iki fonksiyonel derecelendirilmiş (FD) plaka arasında sandviç edilmiş auxetik çekirdek katmanlı bir sandviç plakanın serbest titreşim analizi, çeşitli sınır koşulları altında hem analitik hem de nümerik yöntemler kullanılarak gerçekleştirilmiştir. FD plakalar, silikon nitrür (Si₃N₄)-nikel (Ni) seramik-metal matrisli olarak tasarlanmış ve sandviç yapıdaki malzeme kombinasyonu, mekanik ve termal performansını optimize edilmesi amacıyla tercih edilmiştir. Sandviç yapının malzeme özelliklerinin sıcaklığa bağlı olarak değiştiği varsayılmıştır. Bu bağlamda, auxetik çekirdek katman ve FD yüzey plakalarının sıcaklığa duyarlılığı, dinamik analizlerde dikkate alınmıştır. Yüzey plakalarının efektif malzeme özellikleri, kuvvet yasası dağılımı ile tanımlanmıştır. Bu yaklaşım, malzeme özelliklerinin konuma bağlı olarak değiştiği gerçekçi bir modelleme sağlamaktadır. Sandviç plakanın hareket denklemleri Hamilton prensibi kullanılarak elde edilmiş, serbest titreşim analizinde ise sonlu elemanlar yöntemi (SEY) ve Navier yöntemi kullanılmıştır. Yapılan simülasyon çalışmaları, sandviç plakanın serbest titreşim davranışını etkileyen önemli parametreleri detaylı bir şekilde incelemiştir. Sıcaklık değişiminin plakanın malzeme özelliklerini ve titreşim frekanslarını etkilediği gözlemlenmiştir. Ayrıca, yüzey plakalarının kuvvet yasası indeksindeki değişimlerin, titreşim davranışı üzerinde belirgin bir etkisi olduğu görülmüştür. Auxetik çekirdek katmanının geometrik parametreleri (örneğin, hücre boyutu ve duvar açıları), plakanın genel rijitliğini ve titreşim modlarını önemli ölçüde değiştirmiştir. Analitik ve nümerik yöntemlerden elde edilen sonuçlar kıyaslanmış ve birbirini doğrular nitelikte bulunmuştur. Bu durum, kullanılan yöntemlerin geçerliliğini ve doğruluğunu ortaya koymuştur. Analiz sonuçlarına göre, sıcaklık değişimi, kuvvet yasası parametreleri ve auxetik çekirdek katman geometrisinin plakanın serbest titreşim davranışını önemli ölçüde etkilediği belirlenmiştir. Özellikle, plakanın kullanılacağı ortam koşullarına göre bu parametrelerin optimize edilmesiyle, daha verimli ve güvenilir tasarımların gerçekleştirilebileceği sonucuna ulaşılmıştır. Bu çalışma, auxetik çekirdek katmanlı ve FD yüzey katmanlı sandviç plakalara ilişkin kapsamlı bir titreşim analizi sunarak, gelecekte yapılacak çalışmalar için önemli bir temel sağlamaktadır. Analizlerin doğruluğu ve yöntemlerin uyumu, sandviç yapıların farklı uygulama alanlarında kullanılabilirliğini artıracak yeni tasarımlar geliştirilmesine olanak tanımaktadır. Elde edilen bulguların, havacılık, otomotiv ve denizcilik endüstrileri gibi alanlarda gelişmiş yapıların tasarlanması için değerli bilgiler sağlayacağı düşünülmektedir.

To cite this article:

Aktaş, K. A., & Guvenc, M. A. (2024). Numerical and analytical free vibration analysis of composite plate with auxetic core layer and functionally graded surface layers. *Aerospace Research Letters (ASREL)*, 3(2), 158-174. <https://doi.org/10.56753/ASREL.2024.2.6>

*Corresponding Author: Kerim Gökhan AKTAŞ, kerimgokhanaktas@karabuk.edu.tr



This article is licensed under a Creative Commons Attribution-NonCommercial 4.0 International License (CC BY-NC 4.0)

INTRODUCTION

Auxetic materials, characterized by a negative Poisson's ratio, have gained great interest in recent years due to their unique mechanical properties and potential applications in various areas. The key feature of auxetic materials is their ability to expand laterally when stretched and contract laterally when compressed, which contrasts with conventional materials that exhibit the opposite behavior. This unusual deformation mechanism is due to specific microstructural configurations, such as reentrant geometries or hierarchical structures, which can be designed to optimize performance for desired applications (Critchley et al., 2013; Fan et al., 2018; Gatt et al., 2015). Auxetic core plates exhibit improved mechanical properties, making them appropriate for applications demanding lightweight but stiff materials. Gatt et al. (Gatt et al., 2015) discuss the advantages of hierarchical auxetic mechanical metamaterials that can significantly reduce density while maintaining structural integrity. This property is particularly beneficial in industries such as aerospace and automotive where weight reduction is critical to improve fuel efficiency and performance. Furthermore, Lim's (Lim, 2014) research on auxetic plates on auxetic foundations shows that these materials can effectively damp vibrations and improve wave propagation properties, making them ideal for use in dynamic environments. The unique properties of auxetic materials also extend to their thermal and acoustic behavior. Lim's studies (Lim, 2013b) on thermal stresses in thin auxetic plates show that replacing conventional materials with auxetic solids can significantly reduce thermal stresses, which is advantageous in applications subject to temperature fluctuations. Furthermore, as discussed by Lim (Lim, 2013a), the ability of auxetic structures to control stress wave transmission and reflection demonstrates their potential in applications requiring effective vibration isolation and noise reduction. These properties make auxetic core plates not only mechanically robust but also versatile in various environmental conditions. The study of auxetic materials is not limited to traditional applications; they are also being explored for innovative uses in emerging technologies. For example, the integration of auxetic structures into sensors has been proposed, as their unique deformation properties can improve sensitivity and adaptability in various sensing applications (Dong & Hu, 2023).

Recent studies have shown that auxetic honeycomb structures exhibit improved vibration characteristics compared to their conventional counterparts. For example, Cong et al. (Aktaş, 2024b; Cong et al., 2021) investigated the nonlinear dynamic response of auxetic honeycomb plates subjected to blast loads and highlighted the importance of lattice reinforcements in influencing the vibration behavior. Their findings indicate that the incorporation of auxetic cores can significantly enhance the energy absorption and vibration damping capabilities of sandwich structures. Similarly, Nguyen and Pham Nguyen (Nguyen & Pham, 2016) presented a comprehensive analysis of the nonlinear dynamic response of sandwich composite plates with auxetic honeycombs and emphasized the role of negative Poisson's ratio in enhancing the vibration performance of these materials. Free vibration analysis of auxetic core plates has also been addressed through various computational and experimental methodologies. Tran et al. (T. T. Tran et al., 2020) used a full analytical approach to study the dynamic behavior of sandwich auxetic honeycomb plates on elastic foundations, revealing the complex interaction between core geometry and vibrational properties. Their work underlines the importance of accurately modeling the mechanical properties of auxetic materials to effectively predict their dynamic response. In a complementary study, Stręk et al. (Stręk et al., 2015) focused on the dynamic response of sandwich panels with auxetic cores, providing a detailed investigation of shear deformation and bending stiffness, which are crucial for understanding the vibrational behavior of these structures. Furthermore, the influence of core density and configuration on the dynamic properties of auxetic structures has been the focus of recent research. Essassi et al. (Essassi et al., 2019) performed experimental and numerical analyses to evaluate the dynamic behavior of bio-based sandwich structures with auxetic cores and showed that changes in core density significantly affect the damping properties and vibration

transmission. This finding is in agreement with the observations made by Zhang et al. (Xinchun Zhang et al., 2014) who investigated the dynamic crushing behavior of auxetic honeycombs and highlighted the dependence of in-plane dynamic performance on cell-wall angles and configurations. The integration of advanced modeling techniques such as finite element analysis (FEA) has further improved the understanding of the dynamic response of auxetic core plates. Alavi (Akhavan Alavi & Ghajar, 2024) used modified strain gradient theory to analyze the transient nonlinear response of microcellular auxetic core sandwich plates under impact loads, providing insights into the vibrational properties of these materials under dynamic conditions. The application of FEA in the study of auxetic structures has been validated by numerous researchers, including Zhang and Yang (Xiangwen Zhang & Yang, 2016), who conducted both numerical and experimental studies on auxetic cellular vibration isolation bases, revealing the critical role of Poisson's ratio and relative density in determining the vibration performance. In addition to theoretical and computational approaches, experimental research has also been crucial in verifying the dynamic behavior of auxetic core plates. For example, Zhang et al. (M. Zhang et al., 2024) investigated the low-speed impact response of 3D carbon fiber reinforced polymer auxetic lattice structures and demonstrated the unique failure modes and energy absorption capabilities of auxetic materials. Their findings contribute to the growing body of evidence supporting the use of auxetic structures in applications requiring improved impact resistance and vibration isolation.

The mechanical behavior of auxetic materials is fundamentally different from that of conventional materials. The integration of functionally graded materials (FGMs) into the core structure further enhances the mechanical performance by allowing for tailored properties across the thickness of the sandwich plate, which can be optimized for specific loading conditions (Shi & Shimoda, 2015). For example, Mahesh (Mahesh, 2022) investigated the nonlinear damping properties of auxetic sandwich plates with functionally graded magneto-electro-elastic surfaces under multiphysics loads. The study emphasized the importance of material grading in improving the damping properties and overall structural integrity of sandwich plates. Similarly, Mukahal (Al Mukahal, 2023) investigated the static response of nanocomposite electromagnetic sandwich plates and revealed that the use of functionally graded materials can lead to improved load carrying capabilities and resistance to hygrothermal effects (Dağ, 2024). In addition to mechanical performance, the acoustic properties of functionally graded auxetic core sandwich plates have also been a topic of research. The unique cellular structure of auxetic materials can lead to enhanced sound insulation properties, making them suitable for applications in noise-sensitive environments. For example, Liu et al. (Liu et al., 2019) studied the sound insulation capabilities of pyramidal lattice sandwich structures, highlighting the potential of auxetic designs to contribute to improved acoustic performance in various applications. The fabrication processes of functionally graded auxetic core sandwich plates are also critical to their performance. Advances in additive manufacturing and composite fabrication techniques have enabled the production of complex geometries and specific material distributions required to realize the full potential of these innovative structures (Mastali et al., 2015; Xiong et al., 2016). The ability to control material composition and architecture at different scales allows optimization of mechanical properties and performance characteristics, leading to more efficient and effective designs (Aktaş, 2024a).

The free vibration analysis of composite sandwich plates with metamaterial auxetic core and metal-ceramic FG surface layers has not been analyzed both analytically and numerically with temperature dependent parameters. It is expected that the proposed sandwich structure will make a significant contribution to various application areas such as automotive, aerospace and marine with its high strength-to-weight ratio, high energy absorption capacity, impact resistance, as well as its ability to adapt to thermal and corrosive environments.

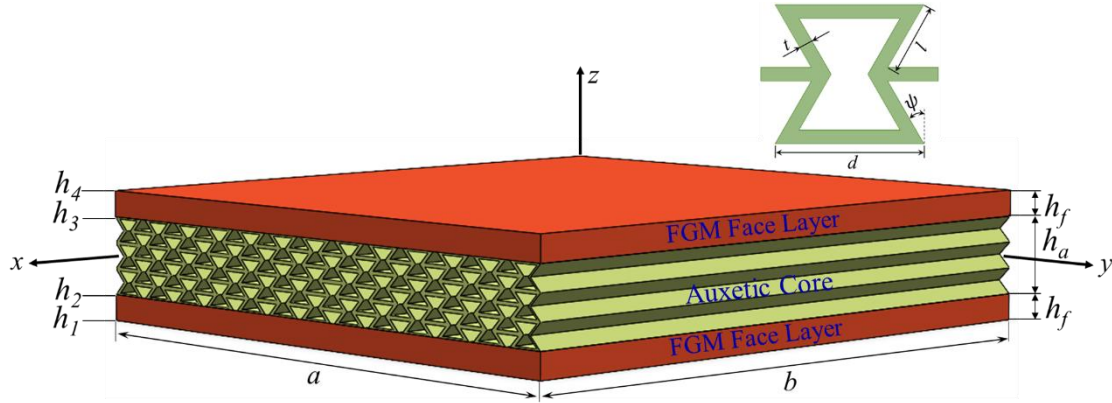
THEORETICAL FORMULATION

Model Description

The re-entrant hexagonal structure is a remarkable example of auxetic metamaterials. As shown in Figure 1, a re-entrant auxetic core structure bonded between two FGM surface layers is considered for the temperature dependent free vibration analysis of the mathematical sandwich structure. Figure 1 also illustrates the unit cell geometry of the re-entrant hexagonal structure. h_a indicates the thickness of the re-entrant auxetic core, while h_f indicates the thickness of the surface layers, which are relatively thinner than the core layer. It is assumed that a thermal load is applied to the sandwich plate in the thickness direction and the temperature propagates nonlinearly through the plate. The re-entrant auxetic core is composed of pure Ni , while the FGM surface plates are composed of Ni/Si_3N_4 matrices where the effective material properties are determined by the power law distribution.

Figure 1

The schematic representation of the proposed auxetic core sandwich plate.



Re-entrant Auxetic Core Configuration

In order to construct the reentrant core layer, auxetic cells are organized in a particular configuration that is determined by inclination angle (ψ), horizontal wall length (d), wall thickness (t) and inclined wall length (l) components. It is possible to compute the mechanical and thermal properties of the auxetic core using the following formula (Li & Yuan, 2022; Nouraei & Zamani, 2023):

$$E_{11}^A = E_{Ni} \left[\frac{(\Upsilon - \sin \psi) \Lambda^3}{[(\Upsilon \sec^2(\psi) + \tan^2(\psi)) \Lambda^2 + 1] \cos^3(\psi)} \right] \quad (1)$$

$$E_{22}^A = E_{Ni} \left[\frac{\Lambda^3}{(\Lambda^2 + \tan^2(\psi)) (\cos(\psi) \Upsilon - \cos(\theta) \sin(\psi))} \right] \quad (2)$$

$$G_{12}^A = G_{Ni} \left[\frac{\Lambda^3}{(2\Upsilon^2 + \Upsilon) \cos \psi} \right] \quad (3)$$

$$G_{13}^A = G_{Ni} \left[\frac{2\sin^2(\psi) + \Upsilon}{2(\Upsilon - \sin(\psi))} + \frac{-\sin(\psi) + \Upsilon}{2\Upsilon + 1} \right] \frac{\Lambda}{2 \cos(\psi)} \quad (4)$$

$$G_{23}^A = G_{Ni} \left[\frac{\Lambda \cos(\psi)}{\Upsilon - \sin(\psi)} \right] \quad (5)$$

$$\rho^A = \rho_{Ni} \left[\frac{(2 + \Upsilon)\Lambda}{2(\Upsilon - \sin(\psi)) \cos(\psi)} \right] \quad (6)$$

$$v_{12}^c = \frac{(\sin(\psi) - \Upsilon)(\sin(\psi))(1 - \beta_3^2)}{\cos^2(\psi) [\Lambda^2(\Upsilon \sec^2(\psi) + \tan^2(\psi)) + 1]} \quad (7)$$

$$v_{21}^c = \frac{(\Lambda^2 - 1) \sin(\psi)}{(\Upsilon - \sin(\psi))(\Lambda^2 + \tan^2(\psi))} \quad (8)$$

$$\alpha_{11}^c = \alpha_{Ni} \frac{\Lambda \cos(\psi)}{\Upsilon + \sin(\psi)} \quad (9)$$

$$\alpha_{22}^c = \alpha_{Ni} \frac{\Lambda(\Upsilon + \sin(\psi))}{(2\Upsilon + 1) \cos(\psi)} \quad (10)$$

in which $\Upsilon = d/l$ and $\Lambda = t/l$.

FGM Surface Layers Effective Properties

The re-entrant core layer is bonded between Ni/Si_3N_4 FGM layers. In this way, the structure is ensured to be lightened without losing its stiffness properties. The top and bottom FGM layers are symmetrical. In other words, the lower surface of the top FGM plate is Ni rich, while the upper surface is Si_3N_4 rich. On the contrary, while the upper surface of the bottom FGM plate is Ni rich, the lower surface is Si_3N_4 rich. Under the influence of the power law exponent, the mechanical and thermal variables of the surface plates exhibit a consistent variation along the thickness direction. In order to determine the functional mechanical and thermal properties of the FGM face plates, the following formula can be utilized (Amini et al., 2015):

$$E_{eff} = E_{Si_3N_4} + (E_{Ni} - E_{Si_3N_4})V^{U,L} \quad (11)$$

$$v_{eff} = v_{Si_3N_4} + (v_{Ni} - v_{Si_3N_4})V^{U,L} \quad (12)$$

$$\rho_{eff} = \rho_{Si_3N_4} + (\rho_{Ni} - \rho_{Si_3N_4})V^{U,L} \quad (13)$$

$$\alpha_{eff} = \alpha_{Si_3N_4} + (\alpha_{Ni} - \alpha_{Si_3N_4})V^{U,L} \quad (14)$$

$$\kappa_{eff} = \kappa_{Si_3N_4} + (\kappa_{Ni} - \kappa_{Si_3N_4})V^{U,L} \quad (15)$$

where the subscripts *eff* represents the effective material characteristics of FGM surface layers. Using the power-law exponent, the volume fraction, represented by $V^{U,L}$, can be found using the following method (Nouraei & Zamani, 2023; Thai & Choi, 2013):

$$V^L = \left(\frac{1}{2} + \frac{2z + h_a + h_f}{2h_f} \right)^n \quad (-h_a/2 - h_f \leq z \leq -h_a/2)$$

$$V^U = \left(\frac{1}{2} - \frac{2z - h_a - h_f}{2h_f} \right)^n \quad (h_a/2 \leq z \leq h_a/2 + h_f) \quad (16)$$

where n denotes the power-law parameter (for $n = 0$, $E_{eff} = E_{Ni}$ and for $n = \infty$, $E_{eff} = E_{Si_3N_4}$). $V^{U,L}$ represents the ratio of *Ni* in the FGM structure. The power-law exponent provides an indicator of the *Ni* content. The volume fraction of metal and ceramic components can be calculated by integrating the distribution over the area. The volume fractions of ceramic and metal components in the FGM surface plates for different power law parameters are illustrated in Table 1.

Table 1

Volume fractions of Ni and Si₃N₄.

Power-law parameter (n)	V_{Ni}	$V_{Si_3N_4}$
0	1.0	0.0
0,5	0.6667	0.3333
1	0.5000	0.5000
2	0.3333	0.6667
5	0.1667	0.8333
10	0.0909	0.9091
20	0.0476	0.9524
100	0.0099	0.9901

In response to changes in temperature, the FGM composite plate exhibits a variety of different mechanical and thermal properties. In order to provide a description of the thermal and mechanical properties, a nonlinear temperature solution can be applied in this way (Reddy & Chin, 1998; Touloukian, 1967; Touloukian YS, 1966):

$$P = P_0(P_{-1}T^{-1} + 1 + P_1T + P_2T^2 + P_3T^3) \quad (17)$$

where $T = T_0 + \Delta T$ and $T_0 = 300$ K. P_0 , P_{-1} , P_1 , P_2 , and P_3 refer to the temperature-dependent material constants. The top and bottom layer temperatures (T_U and T_L) of the plate can be determined as follows: (D. G. Zhang, 2014).

$$-\frac{d}{dz} \left[\kappa(z, T) \frac{dT}{dz} \right] = 0, \quad T \left(\frac{h_a}{2} + h_f \right) = T_U, \quad T \left(-\frac{h_a}{2} - h_f \right) = T_L \quad (18)$$

The temperature of a desired point in the z -axis of the plate can be calculated as follows (Ebrahimi & Barati, 2016):

$$T(z) = T_b + \frac{(T_t - T_b) \int_{-\frac{h}{2}}^z \frac{1}{\kappa(z, T)} dz}{\int_{-\frac{h}{2}}^{\frac{h}{2}} \frac{1}{\kappa(z, T)} dz} \quad (19)$$

Governing Equations

Strain and Displacement

Based on the FSDT, the displacement field (u , v , and w) at any point of the plate element in local axis (x , y , z) can be defined as (V. K. Tran et al., 2020):

$$\begin{aligned} u(x, y, z, t) &= u_0(x, y, t) + z\theta_x(x, y, t) \\ v(x, y, z, t) &= v_0(x, y, t) + z\theta_y(x, y, t) \\ w(x, y, z, t) &= w_0(x, y, t) \end{aligned} \quad (20)$$

where u , v and w are the displacements of any point in the x , y , and z directions. u_0 , v_0 , w_0 , θ_x and θ_y are the displacements of mid-plane and rotation angles of the transverse normal around the y -axis and x -axis, respectively.

From Eq. (20), the normal (ε) and shear strains (γ) can be written as:

$$\begin{bmatrix} \varepsilon_{xx} \\ \varepsilon_{yy} \\ \gamma_{yz} \\ \gamma_{xz} \\ \gamma_{xy} \end{bmatrix} = \begin{bmatrix} \frac{\partial u}{\partial x} \\ \frac{\partial v}{\partial y} \\ \frac{\partial v}{\partial z} + \frac{\partial w}{\partial y} \\ \frac{\partial u}{\partial z} + \frac{\partial w}{\partial x} \\ \frac{\partial u}{\partial y} + \frac{\partial v}{\partial x} \end{bmatrix} = \begin{bmatrix} \frac{\partial u_0}{\partial x} + z \frac{\partial \theta_x}{\partial x} \\ \frac{\partial v_0}{\partial y} + z \frac{\partial \theta_y}{\partial y} \\ \frac{\partial w_0}{\partial y} + \theta_y \\ \frac{\partial w_0}{\partial x} + \theta_x \\ \frac{\partial u_0}{\partial y} + \frac{\partial v_0}{\partial x} + z \left(\frac{\partial \theta_x}{\partial y} + \frac{\partial \theta_y}{\partial x} \right) \end{bmatrix} \quad (21)$$

Constitutive equations

In the classical elasticity theory, stress can be written as follows:

$$\begin{bmatrix} \sigma_{xx} \\ \sigma_{yy} \\ \sigma_{yz} \\ \sigma_{xz} \\ \sigma_{xy} \end{bmatrix}^{C,U,L} = \begin{bmatrix} Q_{11} & Q_{12} & 0 & 0 & 0 \\ Q_{12} & Q_{22} & 0 & 0 & 0 \\ 0 & 0 & Q_{44} & 0 & 0 \\ 0 & 0 & 0 & Q_{55} & 0 \\ 0 & 0 & 0 & 0 & Q_{66} \end{bmatrix} \begin{bmatrix} \varepsilon_{xx} - \alpha T \\ \varepsilon_{yy} - \alpha T \\ \gamma_{yz} \\ \gamma_{xz} \\ \gamma_{xy} \end{bmatrix} \quad (22)$$

where C , U and L represents the auxetic core and surface layers, respectively. Also, Q_{ii} are the stiffness coefficients which can be defined as below (Nouraei et al., 2024):

$$Q_{11} = \frac{E_{11}}{1 - \nu_{12}^2}; Q_{22} = \frac{E_{22}}{1 - \nu_{12}^2}; Q_{12} = \nu_{12}Q_{22}; \quad (23)$$

$$Q_{44}(z) = G_{23}; Q_{55} = G_{13}; Q_{66} = G_{12};$$

It is assumed in the current investigation that $G_{13}=G_{12}$ and $G_{23}= 1.2G_{12}$ (Natarajan et al., 2014).

Hamilton's Principle for Free Vibrational Equations

The free vibrational equations of the sandwich plate can be obtained using the Hamilton's principle as follows:

$$\int_{t_1}^{t_2} (\delta K - \delta U + \delta W) dt = 0 \quad (24)$$

where δK , δU and δW indicate the first variation of the kinetic energy, strain energy, and the work done by the external load, respectively.

The strain energy, denoted by $\delta \mathcal{U}$, is obtained by:

$$\begin{aligned} \delta \mathcal{U} = & \int_{\Omega} \left[\int_{h_1}^{h_2} (\sigma_{xx}^L \delta \varepsilon_{xx} + \sigma_{yy}^L \delta \varepsilon_{yy} + \sigma_{yz}^L \delta \gamma_{yz} + \sigma_{xz}^L \delta \gamma_{xz} + \sigma_{xy}^L \delta \gamma_{xz}) dz \right. \\ & + \int_{h_2}^{h_3} (\sigma_{xx}^C \delta \varepsilon_{xx} + \sigma_{yy}^C \delta \varepsilon_{yy} + \sigma_{yz}^C \delta \gamma_{yz} + \sigma_{xz}^C \delta \gamma_{xz} + \sigma_{xy}^C \delta \gamma_{xz}) dz \\ & \left. + \int_{h_3}^{h_4} ((\sigma_{xx}^U \delta \varepsilon_{xx} + \sigma_{yy}^U \delta \varepsilon_{yy} + \sigma_{yz}^U \delta \gamma_{yz} + \sigma_{xz}^U \delta \gamma_{xz} + \sigma_{xy}^U \delta \gamma_{xz}) dz) \right] dx dy \end{aligned} \quad (25)$$

where $h_1 = -h_a/2 - h_f$, $h_2 = -h_a/2$, $h_3 = h_a/2$ and $h_4 = h_a/2 + h_f$.

δK can be written as:

$$\begin{aligned} \delta \mathcal{K} = & \int_{\Omega} \left[\int_{h_1}^{h_2} \rho^L (\dot{u} \delta \dot{u} + \dot{v} \delta \dot{v} + \dot{w} \delta \dot{w}) dz + \int_{h_2}^{h_3} \rho^C(z) (\dot{u} \delta \dot{u} + \dot{v} \delta \dot{v} + \dot{w} \delta \dot{w}) dz \right. \\ & \left. + \int_{h_3}^{h_4} \rho^U(z) (\dot{u} \delta \dot{u} + \dot{v} \delta \dot{v} + \dot{w} \delta \dot{w}) dz \right] dx dy \end{aligned} \quad (26)$$

The virtual work can be obtained by:

$$\delta W = \int_{\Omega} \left[N_x^T \frac{\partial w_0}{\partial x} \frac{\partial \delta w_0}{\partial x} + N_y^T \frac{\partial w_b}{\partial x} \frac{\partial \delta w_0}{\partial x} \right] dx dy \quad (27)$$

Temperature effects N_x^T and N_y^T are defined by:

$$N_x^T = b \left[\int_{h_1}^{h_2} Q_{11}^L \alpha_L \Delta T dz + \int_{h_2}^{h_3} Q_{11}^C \alpha_C \Delta T dz + \int_{h_3}^{h_4} Q_{11}^U \alpha_U \Delta T dz \right] \quad (28)$$

$$N_y^T = \alpha \left[\int_{h_1}^{h_2} Q_{11}^L \alpha_L \Delta T dz + \int_{h_2}^{h_3} Q_{11}^S \alpha_C \Delta T dz + \int_{h_3}^{h_4} Q_{11}^P \alpha_U \Delta T dz \right] \quad (29)$$

The differential equations that describe the recommended sandwich structure can be obtained by substituting the δU , δK , and δW from equations (25-27) into equation (24).

Solution Procedures

In this study, two different solution methods, analytical and numerical, are employed to solve the equations of motion of a sandwich plate and compared with each other. In order to analyze the natural frequency of the sandwich plate, Navier's method is preferred as the analytical method and finite element method is preferred as the numerical method. ANSYS software is used for finite element analysis of the sandwich plate. The boundary conditions of the presented sandwich plate with simply supported (S), clamped (C) or free (F) edges can be written as follows:

For simply supported (S):

$$v_0 = w_0 = \theta_y = N_{xx} = M_{xx} = 0 \text{ at } x = 0, a \quad (30)$$

$$u_0 = w_0 = \theta_x = N_{yy} = M_{yy} = 0 \text{ at } y = 0, b$$

For clamped (C):

$$u_0 = v_0 = w_0 = \theta_x = \theta_y = 0 \text{ at } x = 0, a; y = 0, b \quad (31)$$

For free (F):

$$M_{xx} = M_{xy} = Q_{xz} = 0 \text{ at } x = 0, a \quad (32)$$

$$M_{yy} = M_{xy} = Q_{yz} = 0 \text{ at } y = 0, b$$

Using the Navier approach, the displacement components can be written as follows considering various boundary conditions (Esen & Özmen, 2022; Sobhy, 2013):

$$\begin{pmatrix} u_0 \\ v_0 \\ w_0 \\ \theta_x \\ \theta_y \end{pmatrix} = \sum_{m=1}^{\infty} \sum_{n=1}^{\infty} \begin{pmatrix} U_{mn} \frac{\partial X_m(x)}{\partial x} Y_n(y) e^{i\lambda t} \\ V_{mn} X_m(x) \frac{\partial Y_n(y)}{\partial y} e^{i\lambda t} \\ W_{mn} X_m(x) Y_n(y) e^{i\lambda t} \\ \theta_{xmn} \frac{\partial X_m(x)}{\partial x} Y_n(y) e^{i\lambda t} \\ \theta_{ymn} X_m(x) \frac{\partial Y_n(y)}{\partial y} e^{i\lambda t} \end{pmatrix}, \quad \alpha = \frac{m\pi}{a}, \beta = \frac{n\pi}{b} \quad (33)$$

where U_{mn} , V_{mn} , W_{mn} , θ_{xmn} and θ_{ymn} define the coefficients of the displacement. Additionally, λ denotes the natural frequency. X_m and Y_n functions are given in Table 2 for different BCs.

Table 2

X_m and Y_n functions for the different BCs.

	BCs		X_m and Y_n functions	
	$x = 0, a$	$y = 0, b$	X_m	Y_n
SSSS	$X_m(0) = X_m''(0) = 0$ $X_m(a) = X_m''(a) = 0$	$Y_n(0) = Y_n''(0) = 0$ $Y_n(b) = Y_n''(b) = 0$	$\sin(\alpha x)$	$\sin(\beta y)$
SSCC	$X_m(0) = X_m''(0) = 0$ $X_m(a) = X_m'(a) = 0$	$Y_n(0) = Y_n''(0) = 0$ $Y_n(b) = Y_n'(b) = 0$	$\sin(\alpha x)$	$\sin^2(\beta y)$
CCCC	$X_m(0) = X_m''(0) = 0$ $X_m(a) = X_m'(a) = 0$	$Y_n(0) = Y_n''(0) = 0$ $Y_n(b) = Y_n'(b) = 0$	$\sin^2(\alpha x)$	$\sin^2(\beta y)$
CSCS	$X_m(0) = X_m'(0) = 0$ $X_m(a) = X_m''(a) = 0$	$Y_n(0) = Y_n'(0) = 0$ $Y_n(b) = Y_n''(b) = 0$	$\sin(\alpha x)[\cos(\alpha x) - 1]$	$\sin(\beta y)[\cos(\beta y) - 1]$

The variables can be written as follows:

$$\{\Delta\} = [U_{mn} \quad V_{mn} \quad W_{mn} \quad \theta_{xmn} \quad \theta_{ymn}]^T \quad (34)$$

The governing equations for the sandwich structure are derived as given below:

$$\{[K] - \lambda_{mn}^2[M]\}\{\Delta\} = 0 \quad (35)$$

where $[K]$ and $[M]$ define the stiffness and mass matrix, respectively.

NUMERICAL RESULTS AND DISCUSSION

In this work, the free vibration analysis of the sandwich plate is carried out numerically in ANSYS FEA software and analytically in MATLAB software using Navier method. The effects of temperature rise, power law index and geometrical parameters of the auxetic structure on the free vibration of the plate are investigated and verified by two different methods. The simulations are based on the following fundamental variables: $a = b = 0.5$ m, $h = a/10$, $h_a = 0.6h$ and $h_f = 0.2h$ ($h = h_a + 2h_f$). The temperature dependent properties of Si_3N_4 and Ni ceramic-metal matrix are listed in Table 3.

Table 3

Mechanical and thermal constants of Ni and Si_3N_4 (Reddy & Chin, 1998; Touloukian, 1967).

Material	Properties	P_{-1}	P_0	P_1	P_2	P_3
Ni	E (Pa)	0	223.95×10^9	-2.794×10^{-4}	3.998×10^{-9}	0
	ν	0	0.31	0	0	0
	α ($1K^{-1}$)	0	9.9209×10^{-6}	8.7050×10^{-4}	0	0
	κ (W/mK)	0	58.754	-4.614×10^{-4}	6.670×10^{-7}	-1.523×10^{-10}
	ρ (kg/m^3)	0	8908	0	0	0
Si_3N_4	E (Pa)	0	348.43×10^9	-3.070×10^{-4}	2.160×10^{-7}	-8.946×10^{-11}
	ν	0	0.24	0	0	0
	α ($1K^{-1}$)	0	5.8723×10^{-6}	9.095×10^{-4}	0	0
	κ (W/mK)	0	13.723	-1.032×10^{-3}	5.466×10^{-7}	-7.876×10^{-11}
	ρ (kg/m^3)	0	2370	0	0	0

Verification of the Proposed Approach

In this section, a validation study is carried out to prove the accuracy of the proposed method. The results of the dimensionless free vibration analysis of the FG plate with Al/Al_2O_3 metal-ceramic matrix are compared with the results of Baferani et al (Hasani Baferani et al., 2011). In the validation study, the values of Modulus of Elasticity, density and Poisson's ratio of Al are considered as $E_m=70$ GPa, $\rho_m=2707$ Kg/m³ and $\nu_m=0.3$ respectively, while the values of Al_2O_3 are considered as $E_c=380$ GPa, $\rho_c=3800$ Kg/m³ and $\nu_c=0.3$. The non-dimensional natural frequency is defined by $\bar{\omega} = \omega h \sqrt{\rho_m/E_m}$. The results of the comparison study for different boundary conditions, power law parameters, and thickness-length ratios are presented in Table 4. As shown in the table, there is a high degree of agreement between the results.

Table 4

Comparison of the dimensionless natural frequency of the FG plate.

BCs	h/a	$n=0.5$		$n=1$		$n=2$	
		Ref.	Present	Ref.	Present	Ref.	Present
SSSS	0.05	0.0249	0.0245	0.0227	0.0222	0.0209	0.0201
	0.1	0.0975	0.0962	0.0891	0.0879	0.0819	0.0802
SFSF	0.05	0.0121	0.0113	0.0109	0.0102	0.0099	0.0088
	0.1	0.0479	0.0479	0.0432	0.0423	0.0393	0.0379
SCSC	0.05	0.0359	0.0356	0.0324	0.0318	0.0295	0.0288
	0.1	0.1366	0.1358	0.1239	0.1231	0.1125	0.1114

Free Vibration Analysis of FG Sandwich Plate

In this subsection, variation of natural frequency (λ) of sandwich FG auxetic core plate with respect to temperature rise (ΔT), power law distribution (n) and auxetic geometrical parameters (Y, Λ and ψ) are investigated in the range of 0-500 K. Analytical and numerical examinations are performed for four distinct power law constants ($n=0, 2, 5,$ and 10). While FG surface plates exhibit completely Ni properties at $n=0$, the plate properties approach Si_3N_4 with increasing n . The analyses are carried out by considering the thickness-to-length of the inclined cell rib ratio $\Lambda = 0.1, 0.2$ and 0.3 , length of the horizontal cell rib-to-length of the inclined cell rib ratio $Y = 2$ and inclination angle $\psi = 30^\circ, 45^\circ$ and 60° .

Table 5 presents the variation of the natural frequency of the sandwich plate with respect to ψ and BCs. In the analysis, four different boundary conditions (CCCC, CCCS, CSCS and SSSS) and three different angle values ($\psi = 30^\circ, 45^\circ$ and 60°) are evaluated. The first three natural frequencies of the sandwich plate are obtained by FEA and Navier method and compared. As shown in the table, the first three natural frequencies of the sandwich plate decrease significantly with increasing theta. It is also found that the natural frequency is significantly affected by varying boundary conditions. The highest natural frequency values are obtained with CCCC while the lowest values are obtained with SSSS boundary conditions. In addition, when the values obtained by numerical and analytical methods are compared, it is seen that the results are quite close.

Table 5

Variation of the natural frequency λ (Hz) with respect to ψ and BCs.

BCs	ψ	Mode 1		Mode 2		Mode 3	
		FE	Navier	FE	Navier	FE	Navier
CCCC	30	348.57	350.47	365.24	368.44	383.34	387.44
	45	310.50	312.82	350.17	353.87	365.08	369.38
	60	284.43	288.56	322.12	325.57	335.56	340.55
CCCS	30	337.94	339.24	346.76	349.12	368.22	371.66
	45	297.20	298.66	328.12	330.88	347.35	352.14
	60	264.04	266.37	296.15	300.03	312.71	317.04
CSCS	30	293.64	295.91	317.32	320.21	329.27	333.83
	45	262.35	264.81	301.23	303.66	312.86	317.96
	60	231.06	232.46	268.24	270.80	279.8	284.92
SSSS	30	192.68	195.78	226.80	230.66	256.12	260.78
	45	169.22	172.65	211.40	214.72	228.91	233.35
	60	148.76	149.86	190.34	193.77	208.78	313.45

The variation of the natural frequency λ of the sandwich plate with respect to parameters ΔT , n and BCs is given in Table 6. As shown in the table, increasing ΔT and n have a decreasing effect on the natural frequency of the plate. The reason for these decreases is that the stiffness of the plate decreases with increasing temperature. The other reason is that with increasing power law index, the material properties of the top and bottom plates approach Si_3N_4 . From Table 3, it is seen that Si_3N_4 is more dominant when Si_3N_4 and Ni modulus of elasticity values are compared. When the boundary conditions are compared, it is found that higher natural frequency values are obtained at CCCC boundary conditions and the difference between Navier and FEA results is smaller.

Table 6

Variation of the natural frequency λ (Hz) with respect to ΔT , n and BCs.

BCs	n	$\Delta T = 100$		$\Delta T = 200$		$\Delta T = 500$	
		FE	Navier	FE	Navier	FE	Navier
CCCC	0	275.48	276.81	257.05	259.26	217.78	220.38
	2	270.12	272.43	253.12	255.38	211.46	213.67
	5	232.50	235.08	216.33	219.22	183.06	186.34
	10	189.78	192.98	176.77	178.89	142.61	146.28
CSCS	0	230.11	232.45	210.22	211.93	167.23	169.38
	2	226.67	229.71	205.43	207.18	162.07	164.87
	5	188.23	193.02	169.27	172.74	127.62	130.69
	10	150.52	153.32	134.92	138.51	109.82	114.23

Table 7 indicates the variations of the natural frequency of the sandwich plate with respect to parameters BCs and Λ . As demonstrated in table, the natural frequency of the sandwich plate increases significantly with increasing Λ . The reason for this increase is that the stiffness of the core plate increases

with increasing thickness. Increasing ΔT and n have an increasing effect on the effective α coefficient of the sandwich plate. The reason for this increase is attributed to the softening tendency of the plate with rising ΔT and the increase in the Si_3N_4 ratio in the surface plates with increasing n .

Table 7

Variation of the natural frequency λ (Hz) with respect to BCs and Λ .

BCs	Λ	Mode 1		Mode 2		Mode 3	
		FE	Navier	FE	Navier	FE	Navier
CCCC	0.1	310.50	313.98	350.17	353.87	365.08	369.38
	0.2	370.38	374.26	415.44	418.21	408.81	411.22
	0.3	450.12	455.32	498.33	502.54	493.32	496.27

CONCLUSIONS

In this paper, the variation of the natural frequency of sandwich structure with auxetic core plate and ceramic-metal matrix FGM surface plates are investigated with respect to variables such as temperature rise, power law index and geometrical parameters of auxetic core cells. To determine the effective equivalent material characteristics of the sandwich plate, power law equations are employed for FG surface plates. According to the parametric analyses, some important outcomes are obtained. When the effect of ΔT , n , ψ , Λ and BCs parameters on the natural frequency of the sandwich plate is examined, it is determined that λ decreases with increasing ΔT , ψ and n , whereas it increases with increasing Λ . Furthermore, it has been found that the parameter providing the greatest influence on the natural frequency of the sandwich plate is the ΔT , whereas the parameter with the least impact is ψ . In addition, when the percentage increases and decreases of the λ of the sandwich structure are examined, it is determined that auxetic cell parameters are more dominant than the other parameters. When the effect of different boundary conditions on the natural frequency of the plate is analyzed, it is found that the highest natural frequency values are obtained with CCCC, and the lowest natural frequency values are obtained with SSSS. The thermomechanical characteristics of sandwich plates including a honeycomb core can be improved via selection of materials and structural design, enabling efficient thermal and mechanical management in high-temperature, noise, and corrosion environments. The results are expected to contribute to the gap in the literature on the current research topic.

Ethical Committee Approval

This study did not use human or animal subjects that require ethics committee approval. The research was conducted on publicly available data sets, literature reviews or theoretical analyses. In accordance with ethical rules, academic integrity and scientific ethics were fully complied with at every stage of the research process. Therefore, ethics committee approval was not required.

Author Contributions

Research Design (CRediT 1) Yazar 1 (%60) – Yazar 2 (%40)

Data Collection (CRediT 2) Yazar 1 (%60) – Yazar 2 (%40)

Research - Data Analysis - Validation (CRediT 3-4-6-11) Yazar 1 (%50) – Yazar 2 (%50)

Writing of the Article (CRediT 12-13) Yazar 1 (%60) – Yazar 2 (%40)

Text Revision and Improvement (CRediT 14) Yazar 1 (%60) – Yazar 2 (%40)

Funding

There is no financial support for the study.

Conflict of Interest

There is no conflict of interest.

Sustainable Development Goals (SDG)

Sürdürülebilir Kalkınma Amaçları: Desteklemiyor

REFERENCES

- Akhavan Alavi, S. M., & Ghajar, R. (2024). Transient Nonlinear Responses of a Sandwich Plate With Micro-Cellular Auxetic Core Based on Modified Strain Gradient Theory Under Impact Loads. *Journal of Sandwich Structures & Materials*, 26(5), 679–702. <https://doi.org/10.1177/10996362241226981>
- Aktaş, K. G. (2024a). 3D wave dispersion analysis of graphene platelet-reinforced ultra-stiff double functionally graded nanocomposite sandwich plates with metamaterial honeycomb core layer. *Mechanics of Time-Dependent Materials*, 28(3), 1873–1908. <https://doi.org/10.1007/s11043-024-09726-z>
- Aktaş, K. G. (2024b). Three-dimensional thermomechanical wave propagation analysis of sandwich nanoplate with graphene-reinforced foam core and magneto-electro-elastic face layers using nonlocal strain gradient elasticity theory. *Acta Mechanica*, 235(9), 5587–5619. <https://doi.org/10.1007/s00707-024-04001-1>
- Al Mukahal, F. H. H. (2023). Static Response of Nanocomposite Electromagnetic Sandwich Plates with Honeycomb Core via a Quasi 3-D Plate Theory. *Mathematics*, 11(9). <https://doi.org/10.3390/math11092046>
- Amini, Y., Emdad, H., & Farid, M. (2015). Finite element modeling of functionally graded piezoelectric harvesters. *Composite Structures*, 129, 165–176. <https://doi.org/10.1016/j.compstruct.2015.04.011>
- Cong, P. H., Quyet, P. K., & Duc, N. D. (2021). Effects of Lattice Stiffeners and Blast Load on Nonlinear Dynamic Response and Vibration of Auxetic Honeycomb Plates. *Proceedings of the Institution of Mechanical Engineers Part C Journal of Mechanical Engineering Science*, 235(23), 7192–7211. <https://doi.org/10.1177/0954406221992797>
- Critchley, R., Corni, I., Wharton, J. A., Walsh, F. C., Wood, R. J. K., & Stokes, K. R. (2013). A Review of the Manufacture, Mechanical Properties and Potential Applications of Auxetic Foams. *Physica Status Solidi (B)*, 250(10), 1963–1982. <https://doi.org/10.1002/pssb.201248550>
- Dağ, T., Güvenç, M. A., & Uyaner, M. (2024). Low Velocity Impact Behavior of Curved Composite Panels Reinforced with Different Types of Stiffeners Used in Air Vehicle. *Journal of Materials and Mechatronics: A*.
- Dong, S., & Hu, H. (2023). Sensors Based on Auxetic Materials and Structures: A Review. *Materials*, 16(9), 3603. <https://doi.org/10.3390/ma16093603>
- Ebrahimi, F., & Barati, M. R. (2016). Electromechanical buckling behavior of smart piezoelectrically actuated higher-order size-dependent graded nanoscale beams in thermal environment. *International Journal of Smart and Nano Materials*, 7(2), 69–90. <https://doi.org/10.1080/19475411.2016.1191556>
- Esen, I., & Özmen, R. (2022). Free and forced thermomechanical vibration and buckling responses of functionally graded magneto-electro-elastic porous nanoplates. *Mechanics Based Design of Structures and Machines*, 0(0), 1–38. <https://doi.org/10.1080/15397734.2022.2152045>
- Essassi, K., Rebière, J.-L., Mahi, A. El, Souf, M. A. Ben, Bouguecha, A., & Haddar, M. (2019). Experimental and Numerical Analysis of the Dynamic Behavior of a Bio-Based Sandwich With an Auxetic Core. *Journal of Sandwich Structures & Materials*, 23(3), 1058–1077. <https://doi.org/10.1177/1099636219851547>

- Fan, D., Li, M., Qiu, J., Xing, H., Jiang, Z., & Tang, T. (2018). Novel Method for Preparing Auxetic Foam From Closed-Cell Polymer Foam Based on the Steam Penetration and Condensation Process. *Acs Applied Materials & Interfaces*, *10*(26), 22669–22677. <https://doi.org/10.1021/acsami.8b02332>
- Gatt, R., Mizzi, L., Azzopardi, J. I., Azzopardi, K. M., Attard, D., Casha, A., Briffa, J. E., & Grima, J. N. (2015). Hierarchical Auxetic Mechanical Metamaterials. *Scientific Reports*, *5*(1). <https://doi.org/10.1038/srep08395>
- Hasani Baferani, A., Saidi, A. R., & Ehteshami, H. (2011). Accurate solution for free vibration analysis of functionally graded thick rectangular plates resting on elastic foundation. *Composite Structures*, *93*(7), 1842–1853. <https://doi.org/10.1016/j.compstruct.2011.01.020>
- Li, F., & Yuan, W. (2022). *Free vibration and sound insulation of functionally graded honeycomb sandwich plates*. <https://doi.org/10.1177/10996362211020440>
- Lim, T. (2013a). Stress Wave Transmission and Reflection Through Auxetic Solids. *Smart Materials and Structures*, *22*(8), 84002. <https://doi.org/10.1088/0964-1726/22/8/084002>
- Lim, T. (2013b). Thermal Stresses in Thin Auxetic Plates. *Journal of Thermal Stresses*, *36*(11), 1131–1140. <https://doi.org/10.1080/01495739.2013.818896>
- Lim, T. (2014). Auxetic Plates on Auxetic Foundation. *Advanced Materials Research*, *974*, 398–401. <https://doi.org/10.4028/www.scientific.net/amr.974.398>
- Liu, J., Chen, T., Zhang, Y., Wen, G., Qing, Q., Wang, H., Sedaghati, R., & Xie, Y. M. (2019). On Sound Insulation of Pyramidal Lattice Sandwich Structure. *Composite Structures*, *208*, 385–394. <https://doi.org/10.1016/j.compstruct.2018.10.013>
- Mahesh, V. (2022). Nonlinear damping of auxetic sandwich plates with functionally graded magneto-electro-elastic facings under multiphysics loads and electromagnetic circuits. *Composite Structures*, *290*(March), 115523. <https://doi.org/10.1016/j.compstruct.2022.115523>
- Mastali, M., Valente, I., Barros, J. A. O., & Gonçalves, D. (2015). Development of Innovative Hybrid Sandwich Panel Slabs: Experimental Results. *Composite Structures*, *133*, 476–498. <https://doi.org/10.1016/j.compstruct.2015.07.114>
- Natarajan, S., Haboussi, M., & Manickam, G. (2014). Application of higher-order structural theory to bending and free vibration analysis of sandwich plates with CNT reinforced composite facesheets. *Composite Structures*, *113*, 197–207. <https://doi.org/10.1016/j.compstruct.2014.03.007>
- Nguyen, D. C., & Pham, C. H. (2016). Nonlinear Dynamic Response and Vibration of Sandwich Composite Plates With Negative Poisson's Ratio in Auxetic Honeycombs. *Journal of Sandwich Structures & Materials*, *20*(6), 692–717. <https://doi.org/10.1177/1099636216674729>
- Nouraei, M., Haghi, P., & Ebrahimi, F. (2024). Modeling dynamic characteristics of the thermally affected embedded laminated nanocomposite beam containing multi-scale hybrid reinforcement. *Waves in Random and Complex Media*, *34*(5), 4122–4151. <https://doi.org/10.1080/17455030.2021.1988758>
- Nouraei, M., & Zamani, V. (2023). *Vibration of smart sandwich plate with an auxetic core and dual-FG nanocomposite layers integrated with piezoceramic actuators*. *315*(February). <https://doi.org/10.1016/j.compstruct.2023.117014>
- Reddy, J. N., & Chin, C. D. (1998). Thermomechanical analysis of functionally graded cylinders and

- plates. *Journal of Thermal Stresses*, 21(6), 593–626.
<https://doi.org/10.1080/01495739808956165>
- Shi, J.-X., & Shimoda, M. (2015). Interface Shape Optimization of Designing Functionally Graded Sandwich Structures. *Composite Structures*, 125, 88–95.
<https://doi.org/10.1016/j.compstruct.2015.01.045>
- Sobhy, M. (2013). Buckling and free vibration of exponentially graded sandwich plates resting on elastic foundations under various boundary conditions. *Composite Structures*, 99, 76–87.
<https://doi.org/10.1016/j.compstruct.2012.11.018>
- Stręk, T., Jopek, H., & Nienartowicz, M. (2015). Dynamic Response of Sandwich Panels With Auxetic Cores. *Physica Status Solidi (B)*, 252(7), 1540–1550.
<https://doi.org/10.1002/pssb.201552024>
- Thai, H. T., & Choi, D. H. (2013). A simple first-order shear deformation theory for the bending and free vibration analysis of functionally graded plates. *Composite Structures*, 101, 332–340.
<https://doi.org/10.1016/j.compstruct.2013.02.019>
- Touloukian, Y. S. (1967). *Thermophysical properties of high temperature solid materials*. Macmillan.
- Touloukian YS. (1966). (1966) *Thermophysical properties of high temperature solid materials. Volume 4. Oxides and their solutions and mixtures. Part 1, vol 1*. Macmillan.
- Tran, T. T., Pham, Q. H., Nguyen-Thoi, T., & Tran, T.-V. (2020). Dynamic Analysis of Sandwich Auxetic Honeycomb Plates Subjected to Moving Oscillator Load on Elastic Foundation. *Advances in Materials Science and Engineering*. <https://doi.org/10.1155/2020/6309130>
- Tran, V. K., Tran, T. T., Phung, M. Van, Pham, Q. H., & Nguyen-Thoi, T. (2020). A Finite Element Formulation and Nonlocal Theory for the Static and Free Vibration Analysis of the Sandwich Functionally Graded Nanoplates Resting on Elastic Foundation. *Journal of Nanomaterials*, 2020. <https://doi.org/10.1155/2020/8786373>
- Xiong, J., Feng, L., Ghosh, R., Wu, H., Wu, L., Ma, L., & Vaziri, A. (2016). Fabrication and Mechanical Behavior of Carbon Fiber Composite Sandwich Cylindrical Shells With Corrugated Cores. *Composite Structures*, 156, 307–319. <https://doi.org/10.1016/j.compstruct.2015.10.009>
- Zhang, D. G. (2014). Thermal post-buckling and nonlinear vibration analysis of FGM beams based on physical neutral surface and high order shear deformation theory. *Meccanica*, 49(2), 283–293.
<https://doi.org/10.1007/s11012-013-9793-9>
- Zhang, M., Li, K., Ho, M. M. P., Etemadi, E., & Hu, H. (2024). Low-velocity Impact Response of 3D Carbon Fiber Reinforced Polymer Auxetic Lattice Structures. *Polymer Composites*, 45(8), 7191–7204. <https://doi.org/10.1002/pc.28259>
- Zhang, Xiangwen, & Yang, D. (2016). Numerical and Experimental Studies of a Light-Weight Auxetic Cellular Vibration Isolation Base. *Shock and Vibration*, 2016, 1–16.
<https://doi.org/10.1155/2016/4017534>
- Zhang, Xinchun, Ding, H. M., An, L. Q., & Wang, X. L. (2014). Numerical Investigation on Dynamic Crushing Behavior of Auxetic Honeycombs With Various Cell-Wall Angles. *Advances in Mechanical Engineering*, 7(2). <https://doi.org/10.1155/2014/679678>